Theory of resistivity upturns in metallic cuprates

W. Chen,[1] Brian M. Andersen,[2] and P. J. Hirschfeld[1]
[1]*Department of Physics, University of Florida, Gainesville, Florida 32611, USA*
[2]*Nano-Science Center, Niels Bohr Institute, University of Copenhagen, Universitetsparken 5, DK-2100 Copenhagen, Denmark*
(Received 10 May 2009; revised manuscript received 19 August 2009; published 23 October 2009)

We propose that the experimentally observed resistivity upturn of cuprates at low temperatures may be explained by properly accounting for the effects of disorder in a strongly correlated metallic host. Within a calculation of the dc conductivity using real-space diagonalization of a Hubbard model treated in an inhomogeneous unrestricted Hartree-Fock approximation, we find that correlations induce magnetic droplets around impurities, and give rise to additional magnetic scattering which causes the resistivity upturn. A pseudogap in the density of states is shown to enhance both the disorder-induced magnetic state and the resistivity upturns.

DOI: 10.1103/PhysRevB.80.134518 PACS number(s): 74.25.Ha, 74.25.Fy, 74.72.−h, 74.81.−g

I. INTRODUCTION

Exotic transport properties in metallic hole-doped cuprates reflect their strongly correlated nature over a large part of their phase diagram. In the vicinity of optimal doping, the in-plane resistivity is found to be linear in temperature T with deviations from linear-T power laws evolving on the underdoped and overdoped sides.[1,2] As the transition temperature T_c is suppressed down to zero by a magnetic field, a resistivity that diverges logarithmically at low temperatures ($\log T$) is observed in $La_{2-x}Sr_xCuO_4$ (LSCO) (Refs. 3 and 4) across a wide range of doping. Resistivity "upturns," increasing ρ as temperature T is decreased below a temperature $T_{\min}$ have been observed as well in $Ba_2Sr_{2-x}La_xCuO_{6+\delta}$ (Refs. 5 and 6) and sufficiently disordered and underdoped $YBa_2Cu_3O_{7-\delta}$ (YBCO) samples.[7–16] Such upturns are frequently associated with a metal-insulator transition as the system approaches its antiferromagnetic (AF) parent compound (for a review, see Ref. 17). However, one should keep in mind that the explanation of these resistivity upturns must include not only the intrinsic electronic correlations present in the system but also their interplay with the external perturbations introduced to suppress superconductivity.

Besides the suppression of T_c, it is known from inelastic neutron-scattering (INS), nuclear-magnetic-resonance (NMR), and muon-spin-rotation (μSR) experiments that introducing disorder and magnetic field can induce local magnetic order, reflecting the coexistence of strong AF correlations with superconductivity. For instance, a strong signal centered at incommensurate positions near (π,π) has been observed in INS experiments in the presence of a magnetic field,[18–21] indicating the formation of AF order around vortices in LSCO; a smaller but significant signal is also present in zero field. Other neutron-scattering measurements have observed evidence of ordered static magnetism in intrinsically disordered cuprates and shown that systematic addition of disorder enhances this effect.[22–25] NMR measurements have furthermore shown evidence that local magnetic moments are induced around atomic scale defects such as Zn substitutions of planar Cu or defects produced by electron irradiation.[17,26–29] The susceptibility of these induced moments shows a Curie-Weiss behavior even though the impurity itself is nonmagnetic, indicating their origin in the strong magnetic correlations present in the pure system. Finally, μSR experiments have shown that the Cu spins freeze in the underdoped superconducting state and eventually develop short-range order at very low temperatures in intrinsically disordered cuprates and even in the much cleaner system YBCO if it is highly underdoped.[30–35] The relationship between ordinary disorder and local magnetism in these and other experiments, has been reviewed in Ref. 17, together with a description of recent theoretical work. Since these phenomena are well established, a theory which seeks to account for the transport anomalies should therefore also be capable of explaining the formation of these local moments, as well as their ordering behavior at different dopings and temperatures.

The logarithmic temperature dependence of the resistivity upturns in a magnetic field has remained a mystery. It is tempting to associate these logs with the quantum corrections to the conductivity found in weak localization theory.[36–38] Indeed, in electron-doped cuprates,[39] where interaction effects are thought to be weaker and disorder effects stronger, as well as in overdoped cuprate samples,[12] good fits of the magnetoresistance data to weak localization theory have been obtained. By contrast, elastic-free paths in hole-doped samples are much larger than the Fermi wavelength scale required for weak localization effects; furthermore the magnetoresistance has the wrong field dependence and typically (but not always[5]) the wrong sign. A $\log T$ behavior of the resistivity is also found in the theory of granular systems[40] but evidence for granularity in the conventional sense is weak or absent in the cuprate samples where the upturns have been observed. Finally, it has been argued by Alloul and others that the body of experimental results on underdoped cuprates, specifically Zn-substituted and irradiation damaged YBCO samples, is consistent with a one-impurity Kondo picture, with conventional resistivity minimum. However there are several inconsistencies associated with this approach reviewed in Ref. 17. We adopt here the alternate point of view that the upturns observed in the underdoped, hole-doped cuprates are manifestations of disorder in a Fermi liquid in the presence of strong antiferromagnetic correlations.

A theory that can cover the anomalies of transport properties in cuprates over a wide range of doping does not currently exist. Recently, an attempt was made to treat disorder

and interactions in a model tailored to the cuprates by Kontani *et al.*[41–43] Within the fluctuation-exchange approach and particular approximations regarding the impurity-scattering processes, these authors had considerable success in reproducing resistivity upturns observed in some cuprates in zero magnetic field. However, as a perturbative approximation it perforce neglects certain self-energy and vertex correction diagrams; in addition, the physical content of the approximations made is not always clear.

Here we focus on the optimally and slightly underdoped cuprates, in the spirit of Kontani *et al.*,[43] and assume the Fermi-liquid picture properly describes the electronic excitations in the normal state. We examine the following simple hypothesis that connects the transport anomalies with the impurity-induced magnetization: the resistivity upturns are due to the extra scattering associated with the correlation-induced magnetic droplets which carry local moments. Within a two-dimensional (2D) single-band Hubbard model where interactions are treated in mean field but disorder is treated exactly, we show that the resistivity increases coincide with the conditions which enhance impurity-induced magnetic moments. The present study focuses on the doping regime where static moments, even in most strongly correlated LSCO, are paramagnetic centers induced by the applied field. Other recent studies relevant to this phase have examined the more disordered, or more correlated state where such magnetic droplets are spontaneously formed around defects in zero field, and shown that they can indeed affect macroscopic observables such as NMR, thermal conductivity and superfluid density $\kappa(T)$.[44–49] The physical picture of the ground state, that of an inhomogeneous mixture of AF droplets carrying net moments near the defect, is quite similar in our case. By working in the regime where moments are smaller and the effect of the field is larger, however, we hope to explain some of the observed puzzling aspects of the magnetoresistance. Since we consider relatively weak correlations, we explicitly confine ourselves to the doping regions in each system under consideration where the resistivity upturns first set in. This means that we, within a self-consistent, unrestricted Hartree-Fock treatment of the correlations, do not expect to be able to describe the true metal-insulator transition or log T behavior, but rather the leading perturbative corrections to the high-T behavior of the resistivity.[50] The conditions in which positive correlations between impurity-induced magnetization and transport anomalies can be found are examined, which confirm our hypothesis that the enhancement of the scattering rate is due to an enlarged cross sections associated with these induced moments. We first examine the case of optimal doping, and then discuss the effect of including a pseudogap in the density of states (DOS), which will allow us to extend the model to lower dopings.

II. MODEL HAMILTONIAN

Since resistivity upturns are typically revealed after T_c is suppressed to zero, the pairing correlation is ignored in describing the normal-state properties as a first approximation. We therefore start with the two-dimensional Hubbard model to describe the CuO_2 plane

$$H = \sum_{ij\sigma} -t_{ij} c_{i\sigma}^{\dagger} c_{j\sigma} + \sum_{i\sigma} (\epsilon_{i\sigma} - \mu)\hat{n}_{i\sigma} + \sum_{i} U\hat{n}_{i\uparrow}\hat{n}_{i\downarrow}, \quad (1)$$

where $c_{i\sigma}$ is the electron operator at site i with spin σ, $\hat{n}_{i\sigma}=c_{i\sigma}^{\dagger}c_{i\sigma}$, $t_{ij}=t,t'$ is the hopping amplitude between nearest-neighbor (t) and next-nearest-neighbor (t') sites, and U is the onsite Coulomb repulsion. The external perturbation due to impurities and magnetic field is included in $\epsilon_{i\sigma}$

$$\epsilon_{i\sigma} = -\frac{1}{2}\sigma g\mu_B B + \sum_r \delta_{ir} V_{imp}, \quad (2)$$

where V_{imp} is the scattering potential produced by defects such as Zn substitution or electronic irradiation. The Zeeman term takes into account the spin-dependent energy shifts caused by the magnetic field with $\sigma=+/-$ for spin up/down, respectively. We will denote $\frac{1}{2}g\mu_B B \equiv B$ in the figures presented below. A Hartree-Fock mean-field decomposition is then adopted to the above Hamiltonian

$$n_i = \langle \hat{n}_{i\uparrow} + \hat{n}_{i\downarrow} \rangle$$

$$m_i = \langle \hat{n}_{i\uparrow} - \hat{n}_{i\downarrow} \rangle, \quad (3)$$

and gives rise to

$$H = \sum_{ij\sigma} -t_{ij} c_{i\sigma}^{\dagger} c_{j\sigma} + \sum_{i\sigma} (\epsilon_{i\sigma} - \mu)\hat{n}_{i\sigma} + \sum_{i\sigma} U\frac{n_i - \sigma m_i}{2}\hat{n}_{i\sigma}. \quad (4)$$

By applying this mean-field ansatz we certainly cannot study Mott correlations in the regime $U \gg t$. We can, however, discuss qualitatively the physics arising from the tendency to form magnetic moments near impurities, as is appropriate near optimal doping. To study the response of the system in a static electric field, we calculate conductivity via linear-response theory, where we use the current in the x direction,

$$J_i = J_i^x = it\sum_{\sigma} (\hat{c}_{i+x\sigma}^{\dagger}\hat{c}_{i\sigma} - \hat{c}_{i\sigma}^{\dagger}\hat{c}_{i+x\sigma}) + it'\sum_{\sigma} (\hat{c}_{i+x\pm y\sigma}^{\dagger}\hat{c}_{i\sigma} - \hat{c}_{i\sigma}^{\dagger}\hat{c}_{i+x\pm y\sigma}), \quad (5)$$

and express the site-dependent current-current correlation function in terms of eigenstates and eigenenergies

$$\pi_{ij}(t) = -i\Theta(t)\langle [J_i(t), J_j(0)] \rangle,$$

$$\pi_{ij}(\omega) = \sum_{n,m} \langle n|J_i|m\rangle\langle m|J_j|n\rangle \frac{f(E_n) - f(E_m)}{\omega + E_n - E_m + i\eta},$$

$$\sigma_i = \sum_j -\lim_{\omega\to 0}\left\{\frac{Im(\pi_{ij}(\omega))}{\omega}\right\} = \pi\sum_j \sum_{n,m} \langle n|J_i|m\rangle\langle m|J_j|n\rangle F(E_n, E_m). \quad (6)$$

The global conductivity σ is realized by averaging σ_i over the whole sample with a proper normalization. The function $F(E_n, E_m)$ is symmetric under exchange of $E_n \leftrightarrow E_m$.[51] The resistivity ρ is then given by the inverse of σ and is plotted in

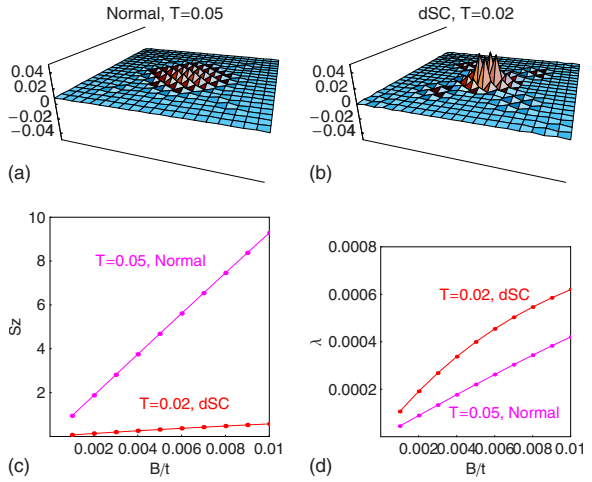

FIG. 1. (Color online) [(a) and (b)] Real-space magnetization pattern induced by a single nonmagnetic impurity for (a) the normal state, and (b) the dSC state, both at $U=1.75$ and $B=0.01$. One sees that the dSC state has more pronounced nearest-neighbor site magnetization due to bound-state formation and has smaller homogeneous magnetization due to the opening of a gap at the Fermi surface. These effects are shown more clearly in (c) the total magnetization S_z and (d) the magnetic contrast λ versus external field.

units of 2D resistivity $\hbar/e^2$. One can also convert it into a three-dimensional (3D) resistivity for materials such as YBCO, in which one assumes two conducting planes per unit cell and gives ρ as 3D resistivity in units of $\hbar/(e^2c)=241\ \mu\Omega$ cm, where c is the average distance between CuO_2 planes and the numerical value given is for YBCO. Note that this procedure gives us only the resistivity part due to impurity scattering; since Hamiltonian (4) is decoupled at the Hartree level, the inelastic processes which may lead to, e.g., the linear resistivity at optimal doping[52] are not treated. We calculate therefore only the low-T part due to elastic scattering.

The proper choice of system size in simulating Eq. (4) is determined by the following criteria. First, in the absence of impurities, homogeneous resistivity ρ_0 should be proportional to the artificial broadening η. Second, the resistivity in the case with impurities should be proportional to the impurity concentration. We found that a 40×40 lattice was sufficient to achieve the above two criteria down to temperature as low as $T_\delta=0.02$, which is roughly equal to the average energy-level spacing, and will be the system size used in the following. Each data point is then averaged over ten different impurity configurations, which we found to be sufficient to ensure the randomness of the impurity distribution. We chose $t'=-0.2$ and the energy unit to be $t=100$ meV, which gives temperature scale $T=0.01t\sim10$ K and the magnetic field scale $B=0.004-7$ T, in the same scale as a recent study of NMR line shapes in the superconducting state.[53]

Before the resistivity under the influence of induced magnetization is studied, we first compare the present study in the normal state with the data in the d-wave superconducting (dSC) state.[53] Such a comparison reveals the importance of finite DOS in the normal state as well as the bound-state formation in the dSC state. The effect of nonmagnetic impurities in the dSC state is studied within the framework of d-wave BCS theory plus magnetic correlations, equivalent to the Hubbard model in Eq. (1) with additional pairing correlations between nearest-neighbor sites $H_{pair}=\Sigma_{i\delta}\Delta_{\delta i}c^\dagger_{i\uparrow}c^\dagger_{i+\delta\downarrow}+\text{H.c.}$, where the gap is to be determined self-consistently $\Delta_{\delta i}=V\langle c_{i\uparrow}c_{i+\delta\downarrow}+c_{i+\delta\uparrow}c_{i\downarrow}\rangle/2$, with $V=1$. The real-space magnetization pattern induced by a single nonmagnetic impurity is shown in Figs. 1(a) and 1(b), where we found three major differences. (1) In the presence of a magnetic field, the normal state has homogeneous magnetization significantly larger than that of the dSC state. This is obviously due to the opening of the gap in the dSC state which reduces the DOS at the Fermi level and hence exhibits a smaller susceptibility than the normal state. (2) The magnetization on the nearest-neighbor sites of the impurity is drastically enhanced in the dSC state, consistent with the bound-state formation due to the d-wave symmetry.[17] (3) The dSC state has a shorter correlation length, resulting from the enhancement of nearest-neighbor site magnetization in comparison with the relatively smaller magnetization on the second- and third-nearest sites away from the impurity. To give a quantitative description of these features, we introduce the total magnetization S_z and the magnetic contrast λ

$$S_z=\sum_i m_i,$$

$$\lambda=\frac{1}{N}\sum_i |m_i-m_0|, \tag{7}$$

where m_i is the magnetization at site i and m_0 is the homogeneous magnetization in the absence of impurities but in the presence of a magnetic field. The meaning of λ is to estimate the fluctuation of site-dependent magnetization away from its homogeneous value m_0, hence an indication of locally induced staggered moment. Since interference between impurities is always present and the local environment is different around each impurity, the deviation from m_0 of the whole system needs to be considered, and therefore we sum over i for λ in Eq. (7). The behavior of S_z and λ versus the applied field is shown in Figs. 1(c) and 1(d), where one sees that S_z in the normal state is one order of magnitude larger than in the dSC state, which is attributed to the overall larger homogeneous susceptibility in the normal state. However, in the λ versus field plot, we see that after the homogeneous magnetization is subtracted, as in the definition of λ, the dSC state has a larger value due to the enhanced magnetization attributed to the bound-state formation. Such a comparison indicates that DOS at the Fermi level is crucial to the formation of impurity-induced moments, which in turn motivates us to propose a phenomenological model that emphasizes the effect of reducing DOS in the underdoped region, as will be discussed in Sec IV.

III. RESISTIVITY UPTURNS AT OPTIMAL DOPING

Motivated by the NMR experiments,[17,26–29] we study the magnetic response in the paramagnetic region close to the magnetic phase boundary. For convenience and direct com-

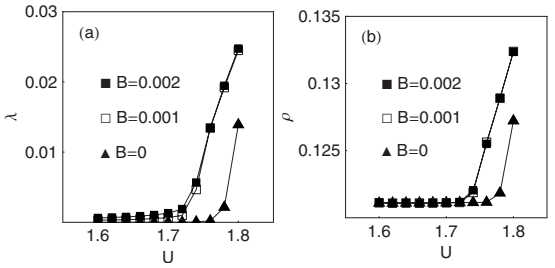

FIG. 2. (a) Magnetic contrast λ and (b) resistivity in units of 241 $\mu\Omega$ cm versus U at optimal doping with $T=0.03$ and 2% impurities.

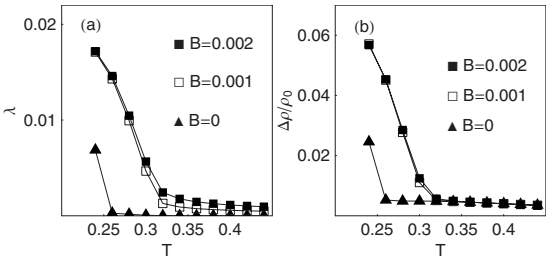

FIG. 3. (a) Magnetic contrast λ and (b) change in resistivity $\Delta\rho/\rho_0$ versus T at optimal doping with $U=1.74$ and 2% impurities.

parison to experiments where unitary scatterers are created by Zn substitution or irradiation defects in YBCO, we choose $V_{imp}=100$. For a system with 2% impurities, we show in Fig. 2(a) the magnetic contrast λ versus U. For the band structure used in this paper, the critical Coulomb repulsion is found to be $U_c \sim 1.75$, above which a spontaneous magnetization is observed for zero field. This value is found to depend on system size and impurity content[53] but the value is roughly close to $U_c \sim 1.75$. As seen in Fig. 2(b),the resistivity increases with U and coincides with the behavior of λ in the region both below and above its critical value. This positive correlation between λ and ρ serves as the first evidence that we can attribute the increase of resistivity to the extra scattering induced by the magnetic moments. In the following discussion we choose $U=1.74$ such that it is close to but slightly below the critical U_c, and the system exhibits paramagnetic response to an external field.

We note that in the region where the system cross the magnetic phase boundary, for instance at large U or low temperatures, numerics found that there are several stable states with comparable energies competing with each other. Taking different initial conditions or a different route for the convergence can result in a different apparent ground-state configuration; for instance, we found a charge-density wave ground state with periodicity (π,π) that can exist in large U and zero field, consistent with the spin- or charge-modulated state found in other studies with a sufficiently large Coulomb repulsion.[45,54–57] However, considering the strong experimental evidence of magnetic ordering, as well as the resulting resistivity in comparison with the transport measurement, only the paramagnetic-induced moment state can give a proper description of both induced magnetization and transport anomalies in the optimal to lightly underdoped systems, and hence will be the stable configuration focused on in this paper.

Due to the limited system size, we are unable to explore the extremely low-T regime, which prevents us from comparing the present theory with the experimentally observed $\log T$ divergence. However, numerics down to as low as $T=0.026-26$ K show significant resistivity upturns in comparison with the zero-field case. Figure 3 shows both magnetic contrast and change in resistivity $\Delta\rho/\rho_0$ versus temperature T, where ρ_0 is the resistivity at the uncorrelated zero-field case $(U=0,\ B=0)$, and one sees again the positive correlation between these two quantities. The lowest temperature explored is slightly lower than the critical temperature $T_{spon} \sim 0.025$ below which a spontaneous magnetization is observed in the zero field. The magnitude of the upturn at $T=0.026$ in comparison with high-temperature resistivity is on the order of 5%, roughly consistent with the value obtained in slightly underdoped YBCO after the inelastic contribution has been subtracted.[8]

The magnetoresistance in the presence of induced magnetization is shown in Fig. 4, where we again see a positive correlation between λ and $\Delta\rho/\rho_0$ with increasing magnetic field B. At the temperatures where the resistivity upturns set in, we found that both λ and $\Delta\rho/\rho_0$ first increase with the field, and eventually saturate and slightly decrease in the high-field region. One can unambiguously define a field scale B_{sat} above which λ and $\Delta\rho/\rho_0$ saturate, and we found that B_{sat} decreases as temperature is lowered. Such a increase-saturation behavior is consistent with the magnetoresistance observed in YBCO,[15,16] although B_{sat} observed therein is slightly higher, possibly due to the higher field required to eliminate the superconductivity before normal-state properties can be observed. Since B_{sat} decreases as lowering temperatures, the region where the magnetic contrast λ is linear with respect to the external field also decreases accordingly, which indicates that as the magnetization starts to grow at low temperatures, the interference between the magnetic islands induced around each impurity is also enhanced, causing λ to deviate from a linear response.

The last issue we need to address is the behavior of λ and $\Delta\rho/\rho_0$ with changing impurity concentration n_{imp}, in comparison with the available experimental data which shows that the resistivity upturns monotonically increase with n_{imp} up to $n_{imp} \sim 3\%$. Figure 5 shows the numerical result under the influence of changing n_{imp}, where one again sees the consistency between the behavior of λ and $\Delta\rho/\rho_0$. However, instead of increasing monotonically with increasing n_{imp}, we found that both λ and $\Delta\rho/\rho_0$ increase up to a critical con-

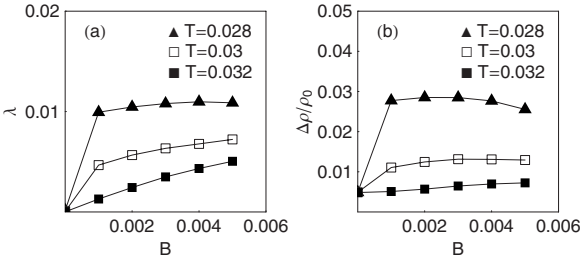

FIG. 4. (a) Magnetic contrast and (b) change in resistivity versus B at optimal doping with $U=1.74$ and 2% impurities.

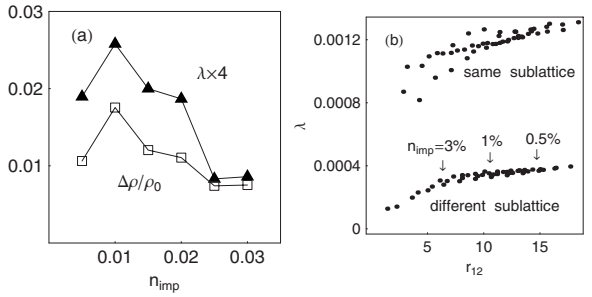

FIG. 5. (a) Magnetic contrast λ and change in resistivity $\Delta\rho/\rho_0$ versus n_{imp} at optimal doping with $U=1.74$, $B=0.001$, $T=0.03$, and (b)λ induced by the two-impurity model plotted against the separation between the two impurities r_{12}, collecting all relative positions up to 13th shell. Values of r_{12} that correspond to average distance of impurities at $n_{imp}=3\%$, 1%, and 0.5% are indicated.

centration $n_{imp}^c \sim 1\%$, and then decrease as more impurities are introduced on the plane. Such a result indicates that the impurity-induced magnetization is proportional to n_{imp} only up to a certain extent, beyond which the interference takes place and eventually destroys the magnetization and the associated magnetic scattering. Note that to further demonstrate that the interference effect is more destructive than constructive to the induced magnetization, we study the two-impurity case in the present model, and plot λ against the separation between the two impurities, as shown in Fig. 5(b). We first found that there exists a strong enhancement of magnetization if both impurities are on the same sublattice, consistent with previous studies in the dSC state.[45,58] Second, λ indeed decreases as the two impurities get closer, which is the case when n_{imp} is increased, indicating the destructive nature of the interference effect, and hence the decreasing of magnetization at sufficiently large impurity content. Our result therefore predicts that if extremely disordered samples ($n_{imp}>3\%$) can be studied experimentally, a critical concentration can occur beyond which the resistivity upturn drops as increasing impurity content, assuming that weak localization has not yet taken place. The critical concentration $n_{imp} \sim 1\%$ shown in the present study is apparently smaller than the experimental value, which may be due to a smaller linear-response region in the present model in comparison with the real cuprates, presumably an artifact of such a weak-coupling mean-field approach. In addition, the critical disorder concentration n_{imp} will depend on the details of the disorder modeling, for instance, the nature of the disorder, or the extent of the impurity potential, which is outside of the scope of our study.

IV. EFFECT OF PSEUDOGAP IN DOS ON RESISTIVITY

From a weak-coupling perspective, we expect enhancement of resistivity upturns as the system is underdoped, based on the following two features: first, correlations are more significant as one approaches half filling, resulting in an increase in the effective U entering our model. Although the Hartree-Fock type mean-field theory cannot capture the Mott transition induced by correlations nor the pseudogap phenomenon, the drastic increase in resistivity near the critical value of U suggests that correlations indeed affect resistivity as one approaches the strong-coupling region. The large U region in Fig. 2 demonstrates that correlation strength U, as well as the induced magnetic moment, are indeed essential ingredients to determine the magnitude of the upturn.

Second, the opening of the pseudogap in the quasiparticle spectrum is known to favor bound-state formation, which in turn promotes the impurity-induced magnetic moment.[17] This is similar to the dSC state where the pole of impurity T matrix falls within the gap, producing a bound state localized around the impurity. We expect that the reduction in the DOS in the pseudogap state also produces poles of the T matrix near the Fermi energy, although the exact form of the Green's function is unknown. Resistivity upturns are then affected by the pseudogap formation based on the naive argument that impurity induced moments result in the upturn. To get a crude idea of the effect of reducing the DOS, we introduce a pseudogap in an *ad hoc* way without going through the T-matrix formalism, since no microscopic model of the pseudogap state is generally agreed upon at present. The following form of dispersion and DOS is proposed for the homogeneous pseudogap state

$$E_k = \mathrm{sign}(\xi_k)\sqrt{\xi_k^2 + \Delta_k^2},$$

$$N(\omega) = \int \frac{dk^2}{4\pi^2} \frac{\eta/\pi}{(\omega - E_k)^2 - \eta^2}, \tag{8}$$

where $\xi_k = -2t[\cos(k_x)+\cos(k_y)] - 4t' \cos(k_x)\cos(k_y) - \mu_f$ is the normal metallic dispersion with a constant "pseudogap" $\Delta_k = 0.2$ and $\eta = 0.1$. We then Fourier transform E_k back to real space and find an effective long-range hopping model that gives the energies E_k. The hopping amplitude t_{ij} of this extended hopping model is therefore

$$t_{ij} = \int \frac{dk^2}{4\pi^2} E_k \{\cos[k_x \cdot (x_i - x_j)] + \cos[k_y \cdot (y_i - y_j)]\}. \tag{9}$$

We calculate the hopping range up to $|x_i - x_j| = |y_i - y_j| = 20$ on a 40×40 lattice. Numerics show a roughly 40% reduction in DOS at the chemical potential, as shown in Fig. 6. The calculation of resistivity then follows Eqs. (5) and (6) while the contribution from all hopping terms $t_\delta = t_{ij}$ and their corresponding distance $\vec{\delta} = \vec{r}_i - \vec{r}_j$ all need to be considered.

Figures 7(a) and 7(b) shows the magnetization and resistivity comparing extended hopping model with the normal-state Hubbard model, Eq. (1), which contains only nearest- and next-nearest-neighbor hopping. We fix both models at optimal doping $\delta = 0.15$ and examine solely the effect of reducing DOS. Within the magnetic field region explored $0 < g\mu_B B/2 < 0.01$, the magnetic contrast λ is found to be enhanced in the extended hopping model, confirming our hypothesis that reducing the DOS promotes bound-state formation, which also gives larger resistance between temperature range $0.02 < T < 0.045$. The magnetization and resistivity versus field is shown in Figs. 7(c) and 7(d), where one sees larger magnetization comparing to the metallic normal-state model, with a smaller linear-response region and the saturation at high field is again revealed. Resistivity upturns

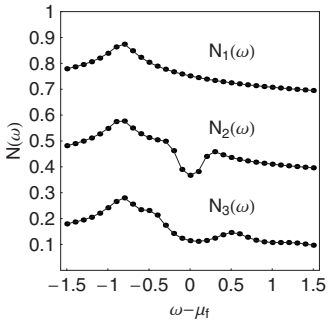

FIG. 6. Comparison of DOS: the normal-state dispersion ξ_k gives $N_1(\omega)$ (shifted), the proposed phenomenological model for the pseudogap state E_k gives $N_2(\omega)$ (shifted), and the actual $N_3(\omega)$ (original scale) given by the effective hopping model after Fourier transform of E_k in a 40×40 system, with $\mu_f=0.02$ and $\Delta=0.2$.

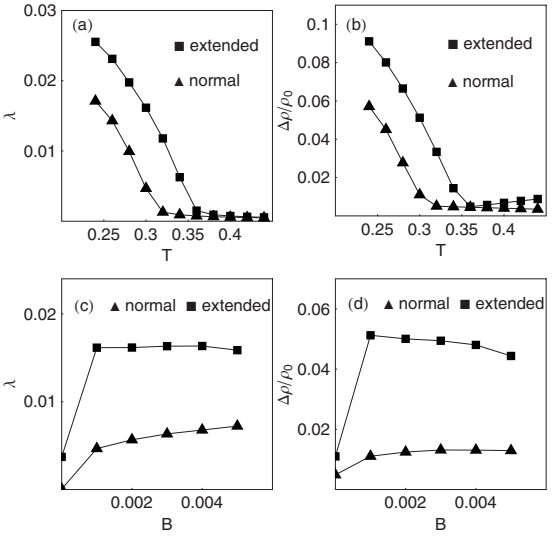

FIG. 7. Comparison of (a) λ and (b) $\Delta\rho/\rho_0$ for models with (extended) and without (normal) reduction in DOS by applying extended hopping Eq. (9), both at optimal doping, with $U=1.75$, $B=0.001$ and 2% impurities. [(c) and (d)]: same quantities vs B for normal and extended hopping models.

are enhanced overall in both low- and high-field regions, and are consistent with the behavior of λ. The hypothesis that reducing the DOS promotes induced moments, and in turn enhances the resistivity upturns, is then substantiated.

V. CONCLUSIONS

In summary, we employed a Hartree-Fock decomposition of the Hubbard model to study transport properties in the cuprates in the presence of disorder-induced magnetization, which is a consequence of the interplay between strong correlations and inhomogeneity. The numerical results suggest that, at low enough temperatures and strong enough correlations, impurity-induced magnetization is drastically enhanced. Within this regime, both induced magnetization and resistivity are increased as (1) the temperature is lowered, (2) the magnetic correlations are enhanced, (3) the magnetic field is increased, and (4) more impurities are introduced, consistent with the conditions in which the enhancement of resistivity is observed experimentally. We predict, in addition, that the addition of further disorder can sometimes lead to a nonmonotonic field dependence as the magnetic potential landscape becomes smooth; this property has not yet been observed to our knowledge. Extremely heavily disordered or strongly correlated samples will lie in a different regime, which we have not yet treated, where disorder will create a spontaneous, short-range ordered magnetic state even in zero field;[45] in this case we anticipate that the magnetoresistance will quite small.

The positive correlation between induced magnetization and resistivity confirms our hypothesis that the enlarged cross section due to these local magnetic moments gives extra scattering and hence the resistivity upturns, consistent with the mechanism previously suggested by Kontani *et al.*,[41–43] and indicates that the hole-doped cuprates lie within this regime over a wide range of (under) doping, in which strong correlations can cause anomalies in the thermodynamic observables. A phenomenological model that produces reduction in DOS near the Fermi level in an *ad hoc* way further suggests that, as the system is underdoped, the anomalous spectrum can promote the impurity bound state and hence the magnetization, which in turn boosts the magnetic scattering and the resistivity upturns. The proposed mean-field theory plus real-space diagonalization scheme is therefore a powerful tool to capture the complex effect on the transport properties due to strong correlations, inhomogeneity, and the spectral anomalies in the low-temperature region where the transport is dominated by disorder. Further applications of the present theory, as well as the influence of impurity-induced magnetization on other thermodynamic observables in the metallic cuprates, will be addressed in a future study.

ACKNOWLEDGMENTS

We appreciate useful discussions with H. Alloul, P. Fournier, L. Taillefer, and F. Rullier-Albenque regarding the interpretation of experiments, and O. P. Sushkov, H. Kontani, D. Maslov, J. Harter, A. T. Dorsey, K. Ingersent, and M. Gabay for various theoretical aspects. Partial funding for this research was provided by DOE-BES under Grant No. DE-FG02-05ER46236. B.M.A. acknowledges support from the Villum Kann Rasmussen foundation. Numerical calculations were performed on the U. Florida High Performance Cluster.

[1] T. R. Chien, Z. Z. Wang, and N. P. Ong, Phys. Rev. Lett. **67**, 2088 (1991).
[2] T. Ito, K. Takenaka, and S. Uchida, Phys. Rev. Lett. **70**, 3995 (1993).
[3] Y. Ando, G. S. Boebinger, A. Passner, T. Kimura, and K. Kishio, Phys. Rev. Lett. **75**, 4662 (1995).

[4] G. S. Boebinger, Y. Ando, A. Passner, T. Kimura, M. Okuya, J. Shimoyama, K. Kishio, K. Tamasaku, N. Ichikawa, and S. Uchida, Phys. Rev. Lett. **77**, 5417 (1996).
[5] Y. Hanaki, Y. Ando, S. Ono, and J. Takeya, Phys. Rev. B **64**, 172514 (2001).
[6] S. Ono, Y. Ando, T. Murayama, F. F. Balakirev, J. B. Betts, and G. S. Boebinger, Phys. Rev. Lett. **85**, 638 (2000).
[7] Y. Fukuzumi, K. Mizuhashi, K. Takenaka, and S. Uchida, Phys. Rev. Lett. **76**, 684 (1996).
[8] K. Segawa and Y. Ando, Phys. Rev. B **59**, R3948 (1999).
[9] K. Segawa and Y. Ando, Phys. Rev. Lett. **86**, 4907 (2001).
[10] D. J. C. Walker, A. P. Mackenzie, and J. R. Cooper, Phys. Rev. B **51**, 15653 (1995).
[11] F. Rullier-Albenque, P. A. Vieillefond, H. Alloul, A. W. Tyler, P. Lejay, and J. F. Marucco, Europhys. Lett. **50**, 81 (2000).
[12] F. Rullier-Albenque, H. Alloul, and R. Tourbot, Phys. Rev. Lett. **87**, 157001 (2001).
[13] F. Rullier-Albenque, H. Alloul, and R. Tourbot, Phys. Rev. Lett. **91**, 047001 (2003).
[14] F. Rullier-Albenque, R. Tourbot, H. Alloul, P. Lejay, D. Colson, and A. Forget, Phys. Rev. Lett. **96**, 067002 (2006).
[15] F. Rullier-Albenque, H. Alloul, F. Balakirev, and C. Proust, Europhys. Lett. **81**, 37008 (2008).
[16] F. Rullier-Albenque, H. Alloul, C. Proust, P. Lejay, A. Forget, and D. Colson, Phys. Rev. Lett. **99**, 027003 (2007).
[17] H. Alloul, J. Bobroff, M. Gabay, and P. J. Hirschfeld, Rev. Mod. Phys. **81**, 45 (2009).
[18] B. Lake, G. Aeppli, K. N. Clausen, D. F. McMorrow, K. Lefmann, N. E. Hussey, N. Mangkorntong, M. Nohara, H. Takagi, T. E. Mason, and A. Schroder, Science **291**, 1759 (2001).
[19] B. Lake, H. M. Rønnow, N. B. Christensen, G. Aeppli, K. Lefmann, D. F. McMorrow, P. Vorderwisch, P. Smeibidl, N. Mangkorntong, T. Sasagawa, M. Nohara, H. Takagi, and T. E. Mason, Nature (London) **415**, 299 (2002).
[20] S. Katano, M. Sato, K. Yamada, T. Suzuki, and T. Fukase, Phys. Rev. B **62**, R14677 (2000).
[21] B. Khaykovich, Y. S. Lee, R. W. Erwin, S.-H. Lee, S. Wakimoto, K. J. Thomas, M. A. Kastner, and R. J. Birgeneau, Phys. Rev. B **66**, 014528 (2002).
[22] H. Kimura, M. Kofu, Y. Matsumoto, and K. Hirota, Phys. Rev. Lett. **91**, 067002 (2003).
[23] T. Suzuki, T. Goto, K. Chiba, T. Shinoda, T. Fukase, H. Kimura, K. Yamada, M. Ohashi, and Y. Yamaguchi, Phys. Rev. B **57**, R3229 (1998).
[24] S. Wakimoto, R. J. Birgeneau, Y. S. Lee, and G. Shirane, Phys. Rev. B **63**, 172501 (2001).
[25] D. Haug, V. Hinkov, A. Suchaneck, D. S. Inosov, N. B. Christensen, Ch. Niedermayer, P. Bourges, Y. Sidis, J. T. Park, A. Ivanov, C. T. Lin, J. Mesot, and B. Keimer, Phys. Rev. Lett. **103**, 017001 (2009).
[26] S. Ouazi, J. Bobroff, H. Alloul, and W. A. MacFarlane, Phys. Rev. B **70**, 104515 (2004).
[27] S. Ouazi, J. Bobroff, H. Alloul, M. Le Tacon, N. Blanchard, G. Collin, M. H. Julien, M. Horvatic, and C. Berthier, Phys. Rev. Lett. **96**, 127005 (2006).
[28] J. Bobroff, W. A. MacFarlane, H. Alloul, P. Mendels, N. Blanchard, G. Collin, and J.-F. Marucco, Phys. Rev. Lett. **83**, 4381 (1999).
[29] J. Bobroff, H. Alloul, W. A. MacFarlane, P. Mendels, N. Blanchard, G. Collin, and J.-F. Marucco, Phys. Rev. Lett. **86**, 4116 (2001).
[30] Ch. Niedermayer, C. Bernhard, T. Blasius, A. Golnik, A. Moodenbaugh, and J. I. Budnick, Phys. Rev. Lett. **80**, 3843 (1998).
[31] C. Panagopoulos, J. L. Tallon, B. D. Rainford, T. Xiang, J. R. Cooper, and C. A. Scott, Phys. Rev. B **66**, 064501 (2002).
[32] T. Adachi, S. Yairi, K. Takahashi, Y. Koike, I. Watanabe, and K. Nagamine, Phys. Rev. B **69**, 184507 (2004).
[33] C. Panagopoulos and V. Dobrosavljević, Phys. Rev. B **72**, 014536 (2005).
[34] S. Sanna, G. Allodi, G. Concas, A. D. Hillier, and R. De Renzi, Phys. Rev. Lett. **93**, 207001 (2004).
[35] R. I. Miller, R. F. Kiefl, J. H. Brewer, Z. Salman, J. E. Sonier, F. Callaghan, D. A. Bonn, W. N. Hardy, and R. Liang, Physica B (Amsterdam) **374-375**, 215 (2006).
[36] B. L. Altshuler and A. G. Aronov, Solid State Commun. **30**, 115 (1979).
[37] B. L. Altshuler, A. G. Aronov, and P. A. Lee, Phys. Rev. Lett. **44**, 1288 (1980).
[38] P. A. Lee and T. V. Ramakrishnan, Rev. Mod. Phys. **57**, 287 (1985).
[39] P. Fournier, J. Higgins, H. Balci, E. Maiser, C. J. Lobb, and R. L. Greene, Phys. Rev. B **62**, R11993 (2000).
[40] I. S. Beloborodov, A. V. Lopatin, V. M. Vinokur, and K. B. Efetov, Rev. Mod. Phys. **79**, 469 (2007).
[41] H. Kontani, K. Kanki, and K. Ueda, Phys. Rev. B **59**, 14723 (1999).
[42] H. Kontani and M. Ohno, Phys. Rev. B **74**, 014406 (2006).
[43] H. Kontani, Rep. Prog. Phys. **71**, 026501 (2008).
[44] G. Alvarez, M. Mayr, A. Moreo, and E. Dagotto, Phys. Rev. B **71**, 014514 (2005); M. Mayr, G. Alvarez, A. Moreo, and E. Dagotto, *ibid.* **73**, 014509 (2006).
[45] B. M. Andersen, P. J. Hirschfeld, A. P. Kampf, and M. Schmid, Phys. Rev. Lett. **99**, 147002 (2007).
[46] W. A. Atkinson, Phys. Rev. B **75**, 024510 (2007).
[47] B. M. Andersen and P. J. Hirschfeld, Physica C **460-462**, 744 (2007).
[48] B. M. Andersen and P. J. Hirschfeld, Phys. Rev. Lett. **100**, 257003 (2008).
[49] G. Alvarez and E. Dagotto, Phys. Rev. Lett. **101**, 177001 (2008).
[50] Note that the self-consistent Hartree-Fock treatment of the Hubbard interaction is equivalent to the random-phase approximation calculation of the induced magnetization.
[51] M. Takigawa, M. Ichioka, and K. Machida, Eur. Phys. J. B **27**, 303 (2002).
[52] T.-P. Choy and P. Phillips, Phys. Rev. Lett. **95**, 196405 (2005).
[53] J. W. Harter, B. M. Andersen, J. Bobroff, M. Gabay, and P. J. Hirschfeld, Phys. Rev. B **75**, 054520 (2007).
[54] J. A. Robertson, S. A. Kivelson, E. Fradkin, A. C. Fang, and A. Kapitulnik, Phys. Rev. B **74**, 134507 (2006).
[55] A. Del Maestro, B. Rosenow, and S. Sachdev, Phys. Rev. B **74**, 024520 (2006).
[56] W. A. Atkinson, Phys. Rev. B **71**, 024516 (2005).
[57] M. Vojta, T. Vojta, and R. K. Kaul, Phys. Rev. Lett. **97**, 097001 (2006).
[58] Y. Chen and C. S. Ting, Phys. Rev. Lett. **92**, 077203 (2004).